ELSEVIER

Biophysical Chemistry 128 (2007) 75–86

Biophysical Chemistry

http://www.elsevier.com/locate/biophyschem

Fluorescence study of protein–lipid complexes with a new symmetric squarylium probe

Valeriya M. Ioffe [a,*], Galyna P. Gorbenko [a], Todor Deligeorgiev [b], Nikolai Gadjev [b], Aleksey Vasilev [b]

[a] *Department of Biological and Medical Physics, V.N. Karazin Kharkov National University, 4 Svobody Sq., Kharkov 61077, Ukraine*
[b] *Department of Applied Organic Chemistry, Faculty of Chemistry, University of Sofia, 1164 Sofia, Bulgaria*

Received 23 January 2007; received in revised form 3 March 2007; accepted 6 March 2007
Available online 13 March 2007

Abstract

The novel symmetric squarylium derivative SQ-1 has been synthesized and tested for its sensitivity to the formation of protein–lipid complexes. SQ-1 binding to the model membranes composed of zwitterionic lipid phosphatidylcholine (PC) and its mixtures with anionic lipid cardiolipin (CL) in different molar ratios was found to be controlled mainly by hydrophobic interactions. Lysozyme (Lz) and ribonuclease A (RNase) exerted an influence on the probe association with lipid vesicles resulting presumably from the competition between SQ-1 and the proteins for bilayer free volume and modification of its properties. The magnitude of this effect was much higher for lysozyme which may stem from the amphipathy of protein α-helix involved in the membrane binding. Varying membrane composition provides evidence for the dye sensitivity to both hydrophobic and electrostatic protein–lipid interactions. Fluorescence anisotropy studies uncovered the restriction of SQ-1 rotational mobility in lipid environment in the presence of Lz and RNase being indicative of the incorporation of the proteins into bilayer interior. The results of binding, fluorescence quenching and kinetic experiments suggested lysozyme-induced local lipid demixing upon protein association with negatively charged membranes with threshold concentration of CL for the lipid demixing being 10 mol%.

Keywords: Squarylium dye; Lysozyme; Ribonuclease A; Protein–lipid interactions; Lipid demixing

1. Introduction

Molecular organization and physicochemical characteristics of biological membranes are influenced by a variety of factors, particularly, by the protein–lipid interactions. Several lines of evidence indicate that peptides and proteins can exert effect on the interfacial electrostatic properties [1,2], degree of phospholipid hydration [3–5], conformation and dynamics of phosphorylcholine group [6,7] and glycerol backbone [8,9]. To address this issue a number of powerful physical techniques have been employed, including NMR [6,7], ESR [4,9], Raman, CD, infrared and fluorescent spectroscopy [3,5,8]. While light scattering hampers CD measurements, Raman spectroscopy misses sensitivity and water absorption affects IR spectra, fluorescence spectroscopy offers rapid, easily-performed, highly sensitive detection relatively independent of the aforesaid processes which limit the use of the other spectroscopic techniques. Little or no damage to the examined sample, requirement of material small amounts, simplicity in methodology, and involvement of relatively inexpensive instrumentation make fluorometry one of the most widely used research tools. The use of specific fluorophores allowed shedding light upon molecular mechanisms of protein–lipid interactions [10–15], protein-induced bilayer reorganizations [16–18], conformational rearrangements of membrane-bound proteins [19,20], structural characterization of protein–lipid complexes and protein orientation in membrane

Abbreviations: NMR, nuclear magnetic resonance; ESR, electron spin resonance; CD, circular dichroism; IR, infrared; PC, egg yolk phosphatidylcholine; CL, cardiolipin; Lz, hen egg white lysozyme; RNase, bovine pancreatic ribonuclease A; RNA, ribonucleic acid; DSC, differential scanning calorimetry; PA, phosphatidic acid; FRET, fluorescence resonance energy transfer; PG, phosphatidylglycerol; *L*:*P*, lipid-to-protein molar ratio; *L*:*D*, lipid-to-dye molar ratio; DPH, 1,6-diphenyl-1,3,5-hexatriene.

* Corresponding author. 32-90 Geroyev Truda St., Kharkov 61146, Ukraine. Tel.: +380 572 658 904, +380 57 343 82 44; fax: +380 57 705 0096.
E-mail address: vioffe@yandex.ru (V.M. Ioffe).

0301-4622/$ - see front matter © 2007 Elsevier B.V. All rights reserved.
doi:10.1016/j.bpc.2007.03.007

plane [21–25], and membrane role in physiological and pathological processes [26–29]. Of particular interest in this context are the probes whose absorption and fluorescence spectra do not overlap with those of the protein or lipid membrane constituents, so that there is no need for correction of fluorescence data for the inner filter and reabsorption [30]. Promising in this respect is the group of squarylium dyes offering a substantial advantage over commonly used dyes due to their absorbance and fluorescence in so-called optical window (600–900 nm) where biological macromolecules are spectroscopically silent. Our previous studies revealed one prospective squarylium probe, largely sensitive to modification of the membrane structure and physical state caused by hydrophobic protein–lipid interactions [31]. To the best of our knowledge, it was one of a few reports about the squaraine probe behavior in highly organized media such as membrane systems. Squarylium dyes have attracted attention mainly because of their potential applications in photoconductor photoreceptor [32], photodynamic therapy [33], optical recording media [34], nonlinear optics [35], and organic solar cells [36]. However, these dyes so far remain poorly examined from the viewpoint of their sensitivity to membrane processes, including protein–lipid interactions. The present study was undertaken to fill this gap. A new squaraine derivative SQ-1, 1,3-disubstituted product synthesized by condensing one equivalent of squaric acid with two equivalents of various types of electron donating carbocycles and heterocycles such as azulene, pyrroles or heterocyclic methylene bases in an azeotropic solvent system, was tested for its sensitivity to the formation of protein–lipid complexes. At the first step of the present study the dye partitioning into the model membranes composed of zwitterionic lipid phosphatidylcholine (PC) and its mixtures with anionic lipid cardiolipin (CL) has been examined. Second step of the study was aimed at evaluating the SQ-1 applicability to monitor the protein-induced changes in lipid bilayer properties. Two single-domain globular proteins, lysozyme (Lz) and ribonuclease A (RNase), whose structure, physicochemical properties and lipid-associating ability are well-characterized to this moment, were chosen as component of the model membrane systems. These proteins are known to be involved in a great number of cellular processes [37–41]. It is becoming widely recognized that central to the functional activities of Lz and RNase is their interactions with membranes. Lysozyme, a hydrolytic enzyme displaying antimicrobial, antitumor and immune modulatory activities has long been a focus of extensive research efforts in numerous fields of inquiry. Lysozyme catalyzes hydrolysis of the β-(1,4)-glycosidic linkage between *N*-acetylglucosamine and muramic acid of the peptidoglycan layer in the bacterial cell wall, thereby promoting cell aggregation and loss of their viability [37]. Accumulating evidence indicates that not only catalytic but also membranotropic properties of lysozyme may account for its bactericidal action [39]. It may be supposed that Lz penetration into the lipid bilayer is responsible for its antimicrobial activity against Gram-positive bacteria. It was shown that Lz increased $^{22}Na^{+}$ permeability of negatively charged vesicles, indicating protein-induced perturbation of lipid bilayer [42]. Ribonuclease A is known mainly for its ability to catalyze the cleavage of single-stranded RNA to yield pyrimidine-2′,3′-cyclic phosphates that are subsequently hydrolyzed to 3′-nucleotides [43]. However, RNase was also reported to interact with the lipid bilayer [44]. Furthermore, utilizing a membrane fraction from hen oviduct, it was found that oligosaccharide–lipid appeared to be a substrate for the glycosylation of ribonuclease A [45]. Along with the conventional functioning, Lz and RNase are involved in pathogenic processes connected with the membrane-initiated and -modulated formation of protein amyloid-like structures which accompany a number of so-called conformational diseases including neurological disorders (Parkinson's, Alzheimer's and Huntington's diseases), type II diabetes, spongiform encephalopathies, systemic amyloidosis, *etc*. [46–52]. All above rationales strongly substantiate the necessity of gaining further insight into molecular details of membrane interactions of Lz and RNase. The choice of PC and CL as lipid components of the examined model systems was dictated by the following reasons. PC is a main component of the most biological membranes. The use of CL as anionic phospholipid seems to be of interest in two main aspects. First, the specificity of Lz–CL interactions. Early ESR studies showed that among the anionic lipids, Lz has the highest affinity for CL with protein selectivity decreasing in the order CL>PG>PS [3]. Second, CL is a membrane constituent of Gram-positive bacteria [53] where Lz exerts its antimicrobial action.

2. Materials and methods

2.1. Materials

Egg yolk phosphatidylcholine and beef heart cardiolipin were purchased from Biolek (Kharkov, Ukraine). Both phospholipids gave single spots by thin layer chromatography in the solvent system chloroform:methanol:acetic acid:water, 25:15:4:2, v/v. Chicken egg white lysozyme was from Sigma (St. Louis, MO, USA). Bovine pancreatic ribonuclease A was from Reanal (Hungary). All other chemicals were of analytical grade.

2.2. Synthesis of SQ-1

2.2.1. Preparation of starting compound **2**

The starting compound **2** was prepared according modified procedure [54] by the quaternization of 2,3,3-trimethyl-benzo[e]indole (**1**) with molar excess of 1-bromobutane (Fig. 1, A). 2 g (0.0096 mol) 2,3,3-trimethyl-benzo[e]indole (**1**) and 2.63 g (2.1 ml, 0.0192 mol) 1-bromobutane were vigorously stirred and heated to 100 °C for 1 h on an oil bath. After cooling to room temperature 20 ml acetone was added. The formed precipitate was suction filtered and dried in a desiccator. Yield 3.2 g (96%). The derived compound is highly hygroscopic and was used without further purification.

2.2.2. Synthesis of the squarylium dye SQ-1

The appropriate squarylium dye SQ-1 (Fig. 1, B) was synthesized according to slightly modified known procedure [55] by the condensation of two fold excess of intermediate **2** and squaric acid in the presence of *N*-ethyl-diisopropylamine as a basic

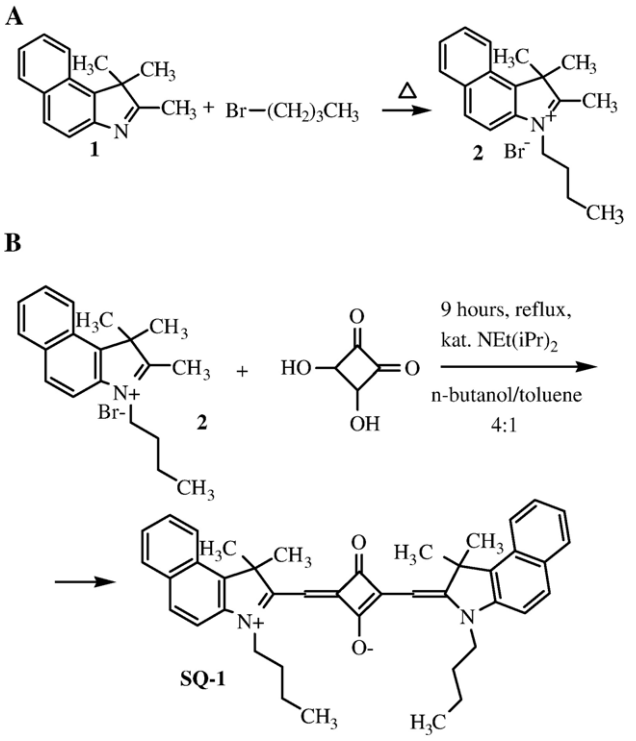

Fig. 1. Preparation of starting compound **2** (A) and synthesis of symmetric squarylium dye SQ-1 (B).

reagent. 0.73 g (0.0021 mol) 1-butyl-2,3,3-trimethyl-benzo[*e*] indolium bromide, 0.11 g (0.001 mol) squaric acid, 0.3 ml *N*-ethyl-diisopropylamine, and mixture of *n*-butanol:benzene=4:1 were mixed in a round-bottomed flask, fitted with magnetical stirrer, reflux condenser and Dean–Stark trap. The reaction mixture was heated under reflux for 9 h with permanent removing of the separated water. After concentration under reduced pressure to half of the initial volume 20 ml diethyl ether was added. The formed precipitate was suction filtered and air dried. The target dye was purified by flash chromatography (methylene chloride/isopropanole=5:1) and with subsequent recrystallization from ethanol. Yield 0.32 g (47%). The chemical structure and the purity of the derived dye were confirmed by ^{1}H NMR spectroscopy and elemental analysis. ^{1}H NMR (DMSO-d_6, δ(ppm)): 0.93–1.023 q (6H, 2×CH_3), 1.39–1.48 m (4H, 2×CH_2), 1.69–1.79 m (4H, 2×CH_2), 1.96 s (12H, 4×CH_3), 4.22 t (4H, 2×NCH_2), 5.88 s (2H, 2×CH), 7.42–8.24 m (12H, Ar). Elemental analysis for $C_{42}H_{44}N_2O_2{\cdot}1.5H_2O$: calc.: C 79.34%, H 7.45%, N 4.41%; found: C 80.08%, 7.10%, N 4.90%. Mp 272–274 °C.

2.3. Preparation of lipid vesicles

Unilamellar lipid vesicles composed of pure PC and PC mixtures with 2.5, 5 or 10 mol% CL were prepared by the extrusion method [56]. Appropriate amounts of lipid stock solutions were mixed in ethanol, evaporated to dryness under a gentle nitrogen stream, and then left under reduced pressure for 1.5 h to remove any residual solvent. The obtained thin lipid films were hydrated with 1.2 ml of 5 mM Na-phosphate buffer (pH 7.4) at room temperature to yield final lipid concentration 10 mM. Thereafter lipid suspensions were extruded through a 100 nm pore size polycarbonate filter (Nucleopore, Pleasanton, CA). The phospholipid concentration was determined according to the procedure of Bartlett [57].

2.4. ^{1}H NMR spectroscopy and elemental analysis

Melting point was determined on a Kofler apparatus and is uncorrected. ^{1}H NMR spectra was obtained on a Bruker 250 MHz instrument in DMSO-d_6. 2,3,3-Trimethyl-benzo[e]indole (**1**), *N*-ethyl-diisopropylamine, squaric acid (**3**) and bromopropane are commercial products and were used as supplied.

2.5. Absorbance and fluorescence measurements

Absorbance and fluorescence measurements were performed at 20 °C with CM 2203 spectrofluorimeter equipped with magnetically stirred, thermostated cuvette holder (SOLAR, Belarus). SQ-1 absorption spectrum was recorded in ethanol, and the concentration of probe ethanolic stock solution was determined using the molar absorptivity $\varepsilon_{663}=2.3\times10^5$ $M^{-1}cm^{-1}$. SQ-1 was used in micromolar concentrations to prevent the dye aggregation. Emission spectra of SQ-1 were recorded in ethanol, buffer and liposomal suspension with excitation wavelength at 660 nm. Excitation and emission band passes were set at 5 nm. Dye fluorescence spectra were recorded at lipid:dye molar ratio varying from 0 to 347.

Steady-state fluorescence anisotropy measurements were performed using excitation and emission wavelengths of 660 and 683 nm, respectively. Excitation and emission slit widths were 10 nm. To incorporate SQ-1 into the model membranes dye–lipid mixtures were incubated for 30 min at room temperature.

Fluorescence quenching experiments were performed with the anionic water soluble quencher iodide. Small aliquots (20 μl) of iodide stock solution (3 M) prepared in 5 mM Na-phosphate buffer (pH 7.4) were added to a stirred and temperature-controlled dye–lipid or dye–lipid–protein mixtures. Ionic strength was kept constant (0.2 M) with the use of KCl. Iodide oxidation was prevented by adding 0.5 M sodium thiosulfate to yield $Na_2S_2O_3$:I^- molar ratio 8:1. The data of the quenching experiments were analyzed according to Stern–Volmer equation [30]:

$$\frac{I_o}{I} = 1 + k_q\tau_o = 1 + K_{SV}[Q] \quad (1)$$

where I_o and I are fluorescence intensities recorded in the absence and presence of a quencher, respectively, k_q is the bimolecular quenching rate constant, τ_o is the fluorophore lifetime in the absence of the quencher, K_{SV} is the Stern–Volmer constant, and $[Q]$ is the quencher concentration.

Fluorescence kinetic experiments were carried out using excitation and emission wavelengths of 660 and 683 nm, respectively. Excitation and emission slit widths were set at 5 nm. Dye–lipid and dye–lipid–protein mixtures were incubated for 30 min at room temperature to achieve lipid-to-dye, lipid-to-lysozyme and lipid-to-ribonuclease molar ratios 227, 93 and 23, respectively.

2.6. Computer-assisted structural analysis

Three-dimensional crystal structures of chicken egg white lysozyme and bovine pancreatic ribonuclease A were generated by WebLab ViewerPro Trial 37 software using the Protein Data Bank files [58,59]. Lysozyme helical wheel presentation was performed by means of WinPep version 3.01.

3. Theory

3.1. Partition model

When the probe binds either to the lipid vesicles or to the protein molecule its total concentration in the sample (Z_{tot}) can be represented as:

$$Z_{tot} = Z_f + Z_{L,P} \tag{2}$$

where Z_f stands for the probe concentration free in bulk solution, Z_L, Z_P are concentrations of the dye, incorporated into the model membranes or bound to the protein, respectively.

The coefficients of dye partitioning into the lipid (K_{PL}) or protein phases (K_{PP}) can be written as [60]:

$$K_P = \frac{Z_{L,P} V_w}{Z_f V_{L,P}} \tag{3}$$

or

$$Z_{L,P} = Z_f K_{PL,PP} \frac{V_{L,P}}{V_w} \tag{4}$$

here V_w, V_L, V_P are the volumes of the aqueous, and lipid or protein phases, respectively. Given that under the employed experimental conditions the volumes of lipid and protein phases are much less than the total volume of the system V_t, we assume that $V_w \approx V_t$ dm^3.

It is easy to show that:

$$Z_f = \frac{Z_{tot}}{1 + K_{PL,PP} V_{L,P}} \tag{5}$$

SQ-1 fluorescence intensity measured at certain lipid or protein concentration can be derived from the following expression:

$$I = a_f Z_f + a_{L,P} Z_{L,P} = Z_f (a_f + a_{L,P} K_{PL,PP} V_{L,P}) \tag{6}$$

where a_f, a_L, a_P represent molar fluorescence of SQ-1 free in solution, and in the lipid or protein environment, respectively.

Inserting Eq. (5) into Eq. (6) one obtains:

$$I = \frac{Z_{tot}(a_f + a_{L,P} K_{PL,PP} V_{L,P})}{1 + K_{PL,PP} V_{L,P}} \tag{7}$$

The volume of lipid phase can be determined from:

$$V_L = N_A C_L \sum v_i f_i \tag{8}$$

where C_L is the molar lipid concentration, f_i is mole fraction of the i-th bilayer constituent, v_i is its molecular volume taken as 1.58 nm^3 and 3 nm^3 for PC and CL, respectively [61]. The volume of the protein phase can be calculated as:

$$V_P = N_A C_P v_P \tag{9}$$

where C_P is the protein molar concentration, and v_P is the volume of fully hydrated protein molecules taken as 2.46 nm^3 for Lz and 3.05 nm^3 for RNase [62]. By examining the fluorescence intensity increase on the probe association with lipids or proteins as a function of lipid or protein concentration the values of K_{PL} and K_{PP} can be derived from Eq. (7).

Similarly, it can be shown that when the probe partitions into protein–lipid system the relationship between its partition coefficients and detected fluorescence intensity can be represented by the following expression:

$$I = \frac{Z_{tot}(a_f + a_L K_{PL} V_L + a_P K_{PP} V_P)}{1 + K_{PL} V_L + K_{PP} V_P} \tag{10}$$

Within the present work the contribution of a_f appeared to be negligibly small, since as indicated below SQ-1 is nearly nonfluorescent in aqueous phase.

The fitting procedure involved minimization of the following error function:

$$\chi^2 = \frac{1}{N} \sum_{i=1}^{N} (I - I_{theor})^2 \tag{11}$$

here N is the number of experimental data points and I_{theor} is SQ-1 fluorescence intensity calculated numerically from the equations underlying the partition model employed.

3.2. Quantum yield calculation

SQ-1 quantum yield (Q_{SQ-1}) was estimated using Cy5 as a standard (Q_{Cy5}=0.28 [63]) according to the relationship:

$$Q_{SQ-1} = \frac{Q_{Cy5}(1 - 10^{-A_{Cy-5}}) S_{SQ-1}}{(1 - 10^{-A_{SQ-1}}) S_{Cy5}} \tag{12}$$

where A_{Cy5} and A_{SQ-1} stand for the absorbance at the excitation wavelength of Cy5 and SQ-1, respectively, S_{Cy5} and S_{SQ-1} are the integrated areas of fluorescence spectra of Cy5 and SQ-1, respectively.

4. Results and discussion

4.1. Spectral properties of SQ-1

As seen in Fig. 1, B, SQ-1 is a symmetric squarylium dye with the central squarate bridge which stabilizes dye chain and helps to increase photostability. Two long butyl tails C_4H_9 connected to nitrogen atoms at the end of the chromophore provide SQ-1 solubility in ethanol and prevent dye aggregation. SQ-1 is zwitterionic probe with positive charge on the nitrogen atom and negative charge on the oxygen one. The dye is characterized by broad absorbance spectrum in the range 550–700 nm with the major peak at 662 nm and the minor one at

614 nm (Fig. 2). SQ-1 was found to exhibit very weak fluorescence in buffer and strong emission in ethanol with strictly defined maximum at 683 nm (Fig. 2). It is also worth noting that the Stokes shift between the SQ-1 absorption and emission spectra in ethanol is relatively small (21 nm) which may indicate that the ground-state and excited-state dipole moments do not significantly differ [30].

4.2. Binding studies

SQ-1 binding to the lipid vesicles is followed by significant increase in fluorescence intensity (Fig. 3, A) and quantum yield from 0.19 for the free dye to 0.57 for lipid-bound SQ-1, while emission maximum was close to that in ethanol (~683 nm), and virtually independent on lipid concentration. This makes SQ-1 an ideal choice as a membrane probe. The enhancement of SQ-1 fluorescence (or quantum yield) in liposomal suspension can be explained by two main factors: (i) the dye transfer to the lipid environment of reduced polarity, and (ii) immobilization of the probe molecules within the lipid bilayer resulting in strongly hindered fluorophore rotation [30,64]. Interestingly, increasing the membrane surface charge by varying cardiolipin (CL) content exerted insignificant effect on the SQ-1 spectral behavior in lipid system (Fig. 3, B) suggesting that dye-membrane association is controlled mainly by hydrophobic interactions. This fact and zwitterionic nature of SQ-1 allowed us to make conclusion about the dye location. It seems likely that zwitterionic in nature SQ-1 chromophore resides in the polar membrane region (approximately at the level of phosphates) while two butyl tails penetrate the hydrophobic region of bilayer and are oriented parallel to the lipid acyl chains. To derive the dye partition coefficients for different lipid systems the experimental dependencies $I(C_L)$ presented in Fig. 3, B were approximated by Eq. (7). The results obtained (Table 1) corroborate the idea that dye–lipid binding is governed by hydrophobic interactions as can be judged from the higher partition coefficient into PC vesicles relative to CL-containing membranes. One may conclude that increasing values of K_{PL} with the increasing concentration of anionic lipid contradict this statement, but, apparently,

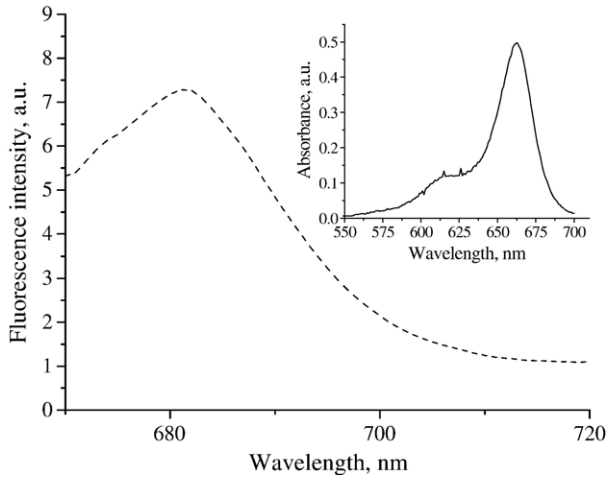

Fig. 2. SQ-1 fluorescence and absorption (shown in inset) spectra.

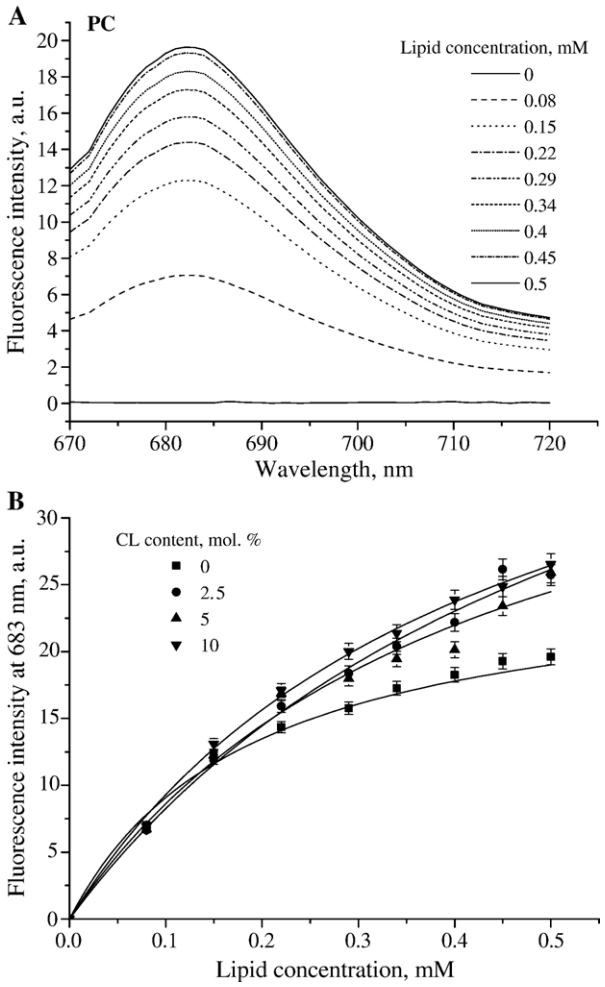

Fig. 3. SQ-1 emission spectra in suspension of PC liposomes (A), and isotherms of SQ-1 binding to PC and PC:CL model membranes (B). Probe concentration was 1.4 μM. Solid lines represent theoretical curves providing the best fit.

the point involves CL effect on the molecular organization of the membrane. According to the studies of Shibata et al. [65], CL is capable to reduce liposome water permeability associated with the bilayer stabilization, the magnitude of this effect increasing with CL content. Probably, this may favor the partitioning of the water insoluble SQ-1 into the membrane.

SQ-1 binding to Lz and RNase resulted in low fluorescence intensity of the probe with the maximum position at 683 nm. Binding isotherms are presented in Fig. 4. SQ-1 binding to Lz and RNase is also mostly hydrophobic because it is expected that forming of electrostatic contacts is not inherent to the zwitterionic dye. SQ-1 partition coefficients into protein phase (K_{PP}) were determined by the approximation of the experimental curves $I(C_P)$ (Fig. 4) by Eq. (7). The obtained results (Table 1) suggest that SQ-1 affinity for RNase is much greater than that for Lz. Notably, K_{PP} is comparable in magnitude with K_{PL}, but molar fluorescence of SQ-1 in the protein phase is much smaller than that in the lipid phase (Table 1). This may be a consequence of the quenching of dye fluorescence by certain protein moieties and lower degree of SQ-1 immobilization within the protein matrix.

4.3. Protein effect on SQ-1 partitioning into the lipid bilayer

The next step of the study was focused on characterization of SQ-1 behavior in the protein–lipid systems. Addition of Lz and RNase to liposomal suspension resulted in the decreased fluorescence intensity of SQ-1 compared to the dye emission in the absence of the proteins (Figs. 3, B and 5). A question arises whether the observed fluorescence changes are caused exclusively by the dye redistribution between the lipid and protein phases. To answer this question it seemed reasonable to quantitatively analyze the dye partitioning into the protein–lipid systems. If only dye redistribution influences SQ-1 emission then measurable fluorescence intensity can be described by Eq. (10). However, as seen in Fig. 6, there is a noticeable discrepancy between theoretical curves calculated from Eq. (10) using K_{PL} and K_{PP} given in Table 1, and the experimental data. This implies that SQ-1 redistribution between protein and lipid phases cannot be considered as the only reason for the observed effects. It seems highly probable that Lz and RNase induce some bilayer perturbations which affect SQ-1 partition into the lipid phase. In this case Eq. (10) takes the form:

$$I = \frac{Z_{tot}(a_L^* K_{PL}^* V_L + a_P K_{PP} V_P)}{1 + K_{PL}^* V_L + K_{PP} V_P} \quad (13)$$

where asterisk allows for the possibility that the partition coefficients and molar fluorescence in the lipidic environment are influenced by protein–lipid interactions. Approximation of the experimental curves by Eq. (13) allowed us to recover the values of $K_{PL}^*$and a_L^*. As seen in Table 1, RNase reduces the values of SQ-1 partition coefficients in all examined lipid systems. Similar in sign but more pronounced in magnitude change was induced by Lz in PC, PC:CL (39:1) and PC:CL (19:1) bilayers. Importantly, the recovered K_{PL}^*values should be considered as reflecting not only modification of bilayer properties *per se*, but also competition between the dye and the protein for bilayer free volume. Proteins' embedment into lipid bilayer may prevent the probe insertion into the membrane interior. RNase exerts less pronounced effect because its ability to penetrate the bilayer is lower than that of Lz. Several lines of evidence from microelectrophoresis, dialysis [42], X-ray diffraction [66], fluorescence polarization [67], surface pressure [68] and isothermal calorimetry [69] measurements strongly emphasize the importance of hydrophobic interactions in lysozyme binding to the phospholipid membranes. According to pioneering classification of Papahadjopoulos, RNase-membrane binding was thought to be mediated only by electrostatic interactions or specific bonds involving non-charged polar groups [70]. The same conclusion has been made on the basis of early permeability studies [42]. However, later results from highly sensitive DSC proved RNase penetration into the lipid phase [71]. Cumulatively, it appears that interactions of soluble proteins like Lz and RNase with the lipid membranes involve two major steps. In a first step, binding is initiated primarily by electrostatic attraction of the cationic protein to the anionic membrane. Next, coverage-dependent penetration of protein molecules into nonpolar bilayer region occurs, followed by interdependent structural alterations of protein and lipid species.

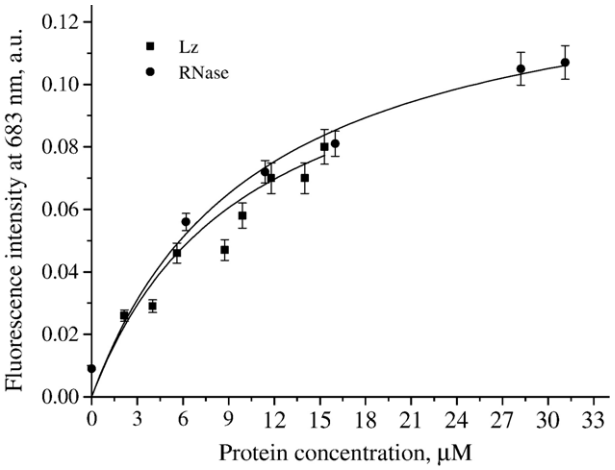

Fig. 4. Fluorescence changes of SQ-1 on the formation of protein–dye complexes. The dye concentration was 1.4 μM. Solid lines represent theoretical curves providing the best fit.

Table 1
Parameters of SQ-1 partitioning into lipid, protein and protein–lipid systems

System		Partition coefficient	Molar fluorescence, M^{-1}	χ^2
PC	No protein	2030±325	$3.3\times10^7\pm510$	0.23
	Lz	951±79	$9.8\times10^7\pm906$	0.18
	RNase	1057±91	$4.1\times10^7\pm215$	0.97
PC:CL (39:1)	No protein	939±97	$7.5\times10^7\pm643$	0.57
	Lz	331±23	$10.1\times10^7\pm1030$	0.14
	RNase	842±86	$8.1\times10^7\pm410$	0.29
PC:CL (19:1)	No protein	1079±147	$6.4\times10^7\pm327$	1.21
	Lz	545±72	$8.4\times10^7\pm807$	0.14
	RNase	701±80	$7.6\times10^7\pm374$	0.36
PC:CL (9:1)	No protein	1468±205	$3.7\times10^7\pm462$	0.74
	Lz	1933±187	$5.9\times10^7\pm334$	0.15
	RNase	1305±401	$4.4\times10^7\pm301$	0.61
Lz	No lipid	876±74	$1.9\times10^5\pm247$	0.74
RNase		2375±271	$9.6\times10^4\pm103$	0.35

The results obtained in the present work also suggest that both hydrophobic and electrostatic protein–lipid interactions may manifest themselves in the change of SQ-1 partition behavior. In particular, in the system PC:CL (9:1)+Lz K_{PL}^* was greater than (Table 1). One possible explanation for this effect involves local lipid demixing upon Lz adsorption on the surface of oppositely charged membranes — charged lipids move toward the protein–lipid binding site in order to minimize the electrostatic free energy of binding. Principle possibility of such effect was demonstrated in DSC study which revealed lateral phase separation in PC:PA vesicles [72]. As followed from our FRET experiments lysozyme binding to the model membranes composed of PC and PG (33 mol%) gave rise to the formation of lipid domains rich in either PC or PG molecules (data not shown). Probably, at CL content 10 mol% electrostatic protein–lipid interactions are strong enough for the lipid segregation to begin — protein binding leads to the formation of membrane domains that consist from the protein and oppositely charged lipid CL. These domains coexist with lysozyme-poor regions

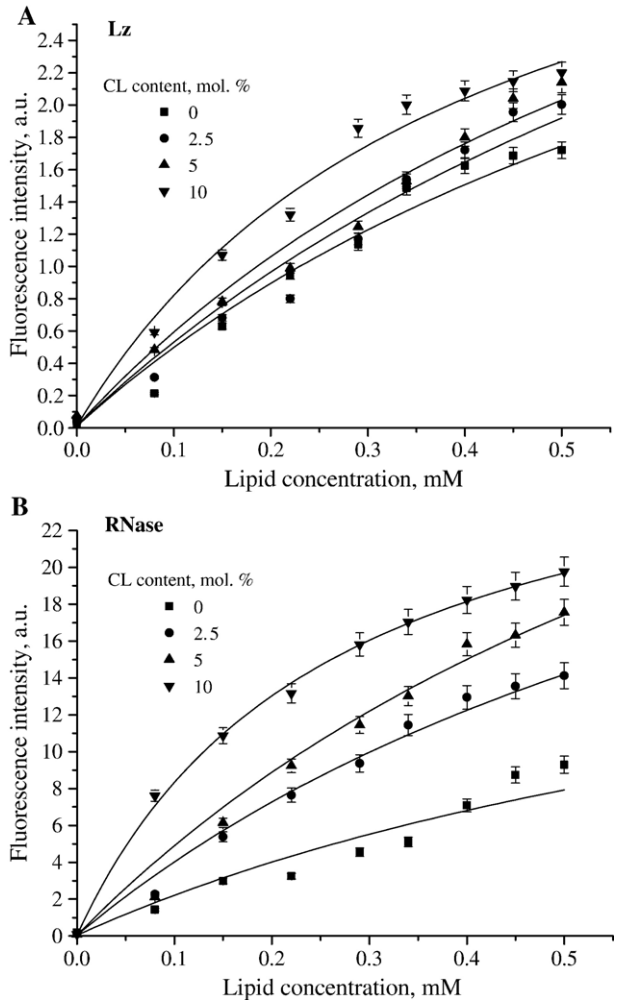

Fig. 5. Lysozyme (A) and ribonuclease A (B) effect on SQ-1 association with lipid vesicles. Fluorescence intensity was measured at 683 nm. The protein concentrations were 4.8 μM (Lz), 11 μM (RNase). SQ-1 concentration was 1.4 μM. Solid lines represent theoretical curves providing the best fit.

which contain a much smaller fraction of charged phospholipids and are formed mainly by PC molecules. This process gains importance with the increase of anionic lipid content and strengthening of the electrostatic protein–lipid interactions. Lz-induced lipid demixing will probably result in the probe lateral redistribution in the bilayer plane. Hydrophobic SQ-1 would prefer PC-rich domains since the highest value of its partition coefficient was observed for the neutral bilayer, while Lz tends to reside in CL-rich regions. This assumption is corroborated by the observation that upon addition of Lz to PC:CL (9:1) liposomes the dye partition coefficient approaches the values of K_{PL} in the neat PC bilayer. Importantly, the process of lipid demixing is controlled by the lipid-to-protein molar ratio (*L*:*P*). Lipid-to-lysozyme ratios employed in our binding studies fall in the range of 17–133. Membrane domain formation gains significance most likely starting from $L{:}P \sim 80$, since at lower *L*:*P* values electrostatic interactions may compete with hydrophobic ones. Moreover, at this point experimental curves tend to reach the plateau region (Fig. 5, A) corresponding to nearly complete dye partitioning into lipid phase observed at lipid-to-dye molar ratio (*L*:*D*) *ca.* 200. In the absence of protein saturable binding was found at *L*:*D a.* 260 (Fig. 3, B). Similarity in these values may be regarded as additional arguments in favor of lipid demixing, starting point for which is approximately $L{:}P \sim 80$. At $L{:}P < 80$ the contribution of electrostatic component of protein–lipid binding is less significant than that of hydrophobic interactions, because bilayer surface potential is significantly reduced. In this case lateral reorganization of membrane into the domains does not produce a considerable change in the electrostatic free energy, and domain formation is energetically unfavorable. At higher *L*:*P* values (>150), when lipid is in excess, protein neutralization of membrane potential is insufficient for overcoming the electrostatic repulsion between negatively charged lipid headgroups, so segregation again becomes unfavorable [73].

Another noteworthy observation concerns the increase of the dye molar fluorescence in the presence of proteins. The changes in this parameter reflect the alterations in the polarity and relaxation characteristics of probe surroundings. Rise in the magnitude of a_L^* is most likely to originate from the protein-

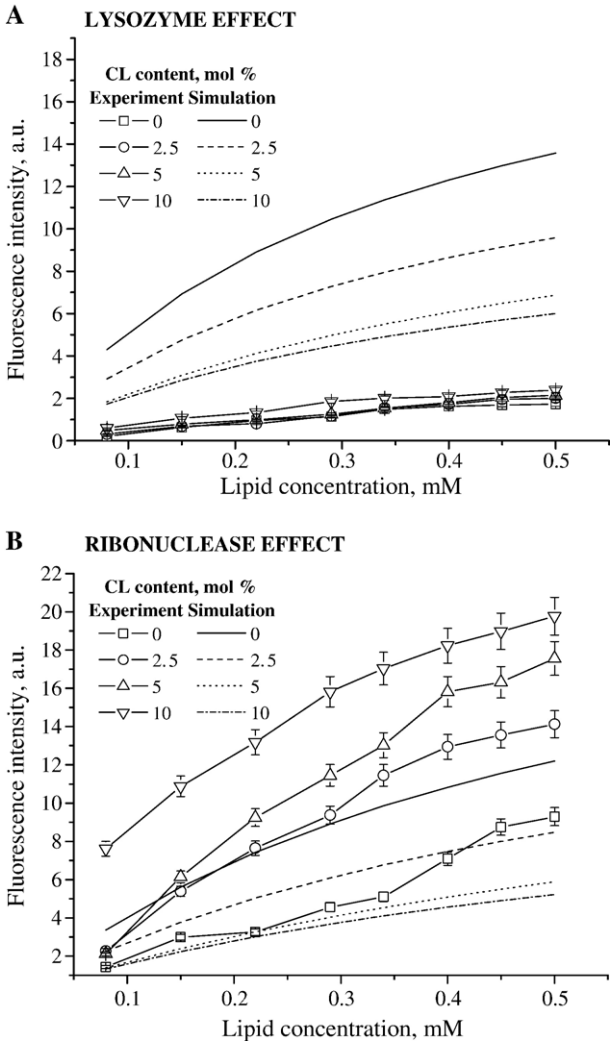

Fig. 6. Distribution of SQ-1 between the lipidic and protein phases: lysozyme (A), ribonuclease A (B). Simulation curves were calculated under the assumption that the parameters K_{PL} and a_L are not influenced by protein–lipid interactions. Concentrations used are: SQ-1 — 1.4 μM, Lz — 4.8 μM, RNase — 11 μM.

induced bilayer dehydration [74]. Again, Lz effect on the probe molar fluorescence was more pronounced compared to RNase, suggesting that the degree of membrane binding of the former protein and extent of subsequent bilayer reorganization is much higher.

4.4. Fluorescence anisotropy studies

To prove that SQ-1 localizes in the bilayer hydrophobic region and responds to the protein incorporation into the membrane, the fluorescence anisotropy measurements have been made. According to the Perrin's concept of rotational depolarization of a fluorophore, the fluorescence anisotropy is correlated with fluidity (or, inversely, microviscosity) of a membrane [30,64]. To determine membrane microviscosity the measured fluorescence anisotropy is compared with the known viscosity of reference solvent [30]. In addition, anisotropy measurements provide information about rotational diffusive motions, the size and shape of macromolecules and intermolecular interactions. While interpreting the anisotropy changes of membrane probes, one should bear in mind that anisotropy values do not in fact accurately reflect the rate of fluorophore rotation in the bilayer, but rather express the extent of the restrictions imposed by the anisotropic lipid environment on the probe motions [64]. Moreover, the terms membrane "fluidity" or "microviscosity" cannot be strictly defined because of highly anisotropic nature of a lipid bilayer whose dynamic properties are controlled by translational, rotational, orientational, and conformational (intramolecular) degrees of freedom of lipid molecules [75]. Since the obligatory prerequisite for all types of motions is the existence of bilayer free volume, it was proposed to use the term "free volume" as more correct than the term "microviscosity" [76]. The membrane free volume characterizes the difference between the effective and van der Waals volumes of lipid molecules. Packing constraints and thermal motion cause *trans-gauche* isomerization of acyl chains, thereby producing dynamic, short-lived defects (kinks) in the hydrocarbon core. A local free volume is generated in a bilayer due to lateral displacement of hydrocarbon chain on the kink formation.

SQ-1 anisotropy remained virtually unchanged upon Lz and RNase association with PC bilayers (Fig. 7). Despite the results of binding experiments presented here are suggestive of hydrophobic interactions of these proteins with uncharged membranes, SQ-1 anisotropy appeared insensitive to protein-induced modification of PC bilayer. Notably, DPH also didn't respond to Lz association with neutral bilayers [77]. As seen in Fig. 7, incorporation of the proteins into CL-containing model membranes in the majority of cases brings about the increase of SQ-1 fluorescence anisotropy. These changes most probably result from the restrictions of the probe rotation induced by the reduction of the membrane free volume upon the penetration of Lz and RNase into the bilayer hydrophobic region. Besides, as indicated above, the binding of these proteins may give rise to bilayer dehydration. Removal of water enhances the interactions between lipid molecules and increases ordering of lipid headgroups [78]. Restrictions imposed by increased packing density of lipid headgroups inhibit the probe photoisomerization and also may hinder its rotation [79–81]. Importantly, SQ-1 anisotropy increases with protein concentration and CL content. This finding implies that enhancement of electrostatic component of protein–lipid binding strengthens the hydrophobic interactions of the proteins with the acyl chains of lipid molecules. Again, the magnitude of the observed effects was greater for lysozyme suggesting higher extent of protein–lipid binding and subsequent bilayer perturbation. Interestingly, the maximum SQ-1 anisotropy increase (about two-fold) was observed in the system Lz+PC:CL (9:1). Obviously, not only lipid ordering results in such significant anisotropy change. Restrictions of the probe rotation may be also caused by Lz aggregation. Our previous studies provided the arguments in favor of protein oligomerization in the lipid environment [Gorbenko, Ioffe, and Kinnunen, to be published]. In brief, based on the results of binding studies, DPH anisotropy measurements and protein intrinsic fluorescence quenching, it was concluded that Lz association with the lipid vesicles is followed by the formation of protein aggregates between bilayer-embedded protein molecules. If this is the case, then protein self-associates would decrease membrane free volume to a higher extent than monomeric species leading to more significant ordering of lipid

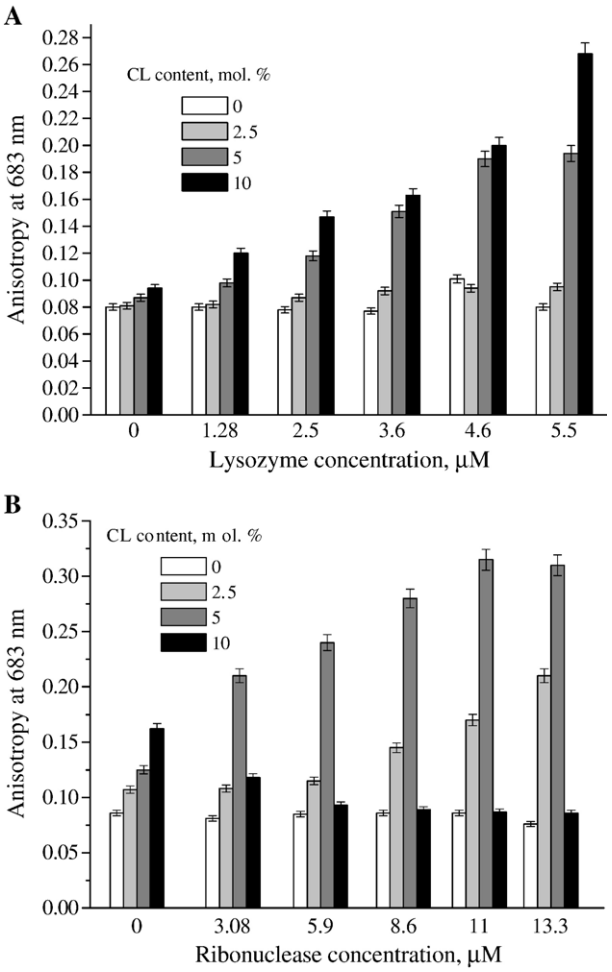

Fig. 7. Fluorescence anisotropy of SQ-1 in protein–lipid systems at varying protein concentrations: lysozyme (A), ribonuclease A (B). Lipid and probe concentrations were 0.08 mM and 1.5 μM, respectively.

molecules and restrictions of SQ-1 rotation. This suggestion is also corroborated by the considerations of protein–lipid geometry and stoichiometry. Theoretical saturation coverage of the lipid vesicle by Lz molecules corresponds to L:P ratio *ca.* 40, or L_o:$P \sim 20$ (L_o is the concentration of lipids in the outer monolayer accessible to lysozyme binding), with the protein cross-section and mean area of phospholipid headgroup taken as 13.5 nm^2 and 0.65 nm^2, respectively [61,62]. L_o:P values employed in our anisotropy measurements range from 8 to 32. It might be expected that at L_o:P<20 the membrane is fully covered with the protein, and subsequent increase in protein concentration and lowering the L_o:P values up to 8 results in Lz adsorption onto the protein monolayer which stretches along the bilayer surface, initiating the aggregation of membrane-bound protein.

RNase-induced decrease in probe anisotropy in PC:CL (9:1) vesicles remains unclear. The main causes of fluorescence depolarization include: (i) non-parallel absorption and emission transition moments, (ii) torsional vibrations, (iii) Brownian motions, (iv) resonance energy transfer, and (v) decrease in size of rotating species [30]. However, we do not see any reasons for the realization of any of these phenomena upon RNase association with PC:CL (9:1) model membranes since the results presented in the previous and further sections didn't point to any specific processes occurring between SQ-1, RNase and this type of bilayer. It is unlikely to be an experimental error because the measurements were repeated three times. It may be supposed analogously to Lz that this effect stems from RNase-induced domain formation since probe anisotropy in PC:CL (9:1) reaches the values of that measured in the neat PC bilayer, but other results presented here didn't confirm this suggestion. Substantiation of this viewpoint invites further investigations.

4.5. Fluorescence quenching studies

To gain further insight into SQ-1 sensitivity to the protein–lipid interactions and their consequences we employed fluorescence quenching technique which may provide essential information on the localization of the fluorophore in the membrane [30,64]. As can be judged from Stern–Volmer constants presented in Table 2, in the absence of proteins the most effective quenching of SQ-1 fluorescence by iodide was observed in CL-containing model membranes relative to the neat PC liposomes. Since iodide is a water soluble anionic quencher these results suggest that in PC bilayer SQ-1 is located deeper than in PC:CL membranes. It should be noted that though iodide is an anion it can permeate the membrane [30,64,82]. Several lines of evidence indicate that iodide quenches the fluorescence of membrane-buried probes [30,83]. The permeation process by which ions and small polar molecules cross phospholipid bilayers, is commonly interpreted in terms of two alternative theories: the solubility–diffusion mechanism and the pore mechanism. According to the solubility–diffusion mechanism, lipid bilayer is considered as a thin slab of a hydrophobic medium that separates two aqueous phases and acts as a diffusion barrier. In order to get from one aqueous phase into the other, the ion must dissolve into the hydrophobic phase, diffuse across it, and dissolve into the second aqueous phase [84]. In the pore mechanism permeation of ions across a bilayer occurs through transient defects that are produced by thermal fluctuations [85]. Paula et al. concluded that the former theory better describes the permeation of halide ions such chloride, bromide and iodide across phospholipid bilayers than the pore mechanism [82]. The detailed consideration of this question is out of the scope of this manuscript and will be discussed elsewhere. We just postulate that the probe accessibility to the iodide is not in conflict with the assumption about SQ-1 location in the bilayer hydrophobic core.

Addition of the proteins resulted in K_{SV} increase in all types of lipid vesicles for RNase and in PC, PC:CL (39:1) and PC:CL (19:1) model membranes for Lz (Table 2). The rise in Stern–Volmer constant is indicative of the protein-induced increase in probe accessibility to the iodide. This effect may be explained by the aforesaid competition between SQ-1 and proteins for the bilayer free volume. Incorporation of the proteins into the membrane hampers SQ-1 partitioning into the lipid phase, so that the dye tends to reside closer to the membrane surface thereby becoming more accessible to the iodide. Intriguingly, Lz association with PC:CL (9:1) liposomes resulted in significant K_{SV} drop. Furthermore, the value of Stern–Volmer constant for this type of membranes was close to that observed for the neat PC vesicles. This result provides convincing argument in favor of the suggestion about Lz-induced lipid demixing and formation of PC- and CL-rich domains. Importantly, at L:P ratio employed in the quenching studies (*ca.* 95) electrostatic lysozyme–lipid interactions seem to be predominant, providing necessary prerequisite for the lipid segregation — screening the electrostatic repulsion between charged lipids followed by enhancement of their attraction and the demixing tendency of the system [73].

4.6. Kinetic studies

At the last step of the study it seemed of interest to ascertain whether Lz and RNase affect the kinetics of SQ-1 association with lipid vesicles. Kinetic experiments have been made with PC:CL (9:1) liposomes because the most pronounced effects of Lz and RNase have been observed for this type of model membranes. As seen in Fig. 8, addition of the proteins slows down the probe binding to the lipid bilayer. Quantitatively this process can be described by the following expression [86]:

$$I = I_{max}\left(1-\exp\left(-\frac{t}{\tau_{eq}}\right)\right) \quad (12)$$

where I is the probe fluorescence intensity measured at time t, I_{max} denotes the limit SQ-1 fluorescence in the lipid environment,

Table 2
Stern–Volmer constants for quenching of SQ-1 fluorescence by iodide in different systems

System	No protein	Lz	RNase	χ^2
PC	0.58±0.03	1.33±0.06	0.61±0.04	0.5
PC:CL (39:1)	1.05±0.05	1.49±0.07	1.36±0.1	0.1
PC:CL (19:1)	0.9±0.06	1.25±0.04	1.24±0.04	0.3
PC:CL (9:1)	1.47±0.1	0.54±0.02	2.06±0.1	0.1

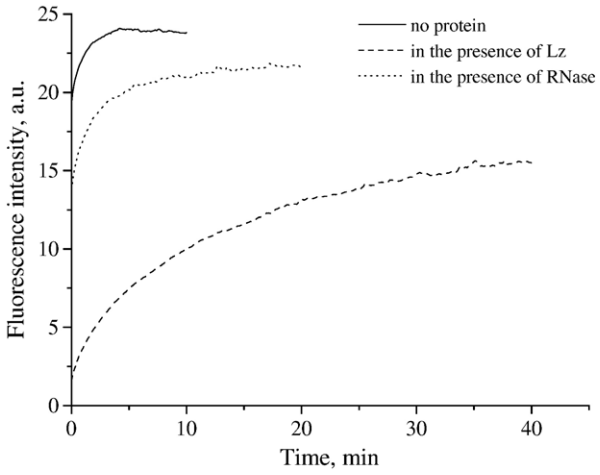

Fig. 8. Time course of SQ-1 binding to the PC:CL (9:1) lipid membranes in the absence of proteins. Concentrations used are: SQ-1 — 1.1 μM, lipid — 0.25 mM, Lz — 2.7 μM, RNase — 11 μM.

τ_{eq} stands for the characteristic time of approaching the thermodynamic equilibrium. Approximation of the experimental curves presented in Fig. 8 by the Eq. (12) yielded kinetic parameters I_{max} and τ_{eq} for lipid and protein–lipid systems. As seen in Table 3, association of the proteins with the lipid vesicles was followed by the increase of τ_{eq} values. This observation confirms the idea about the protein–dye competition for free volume of the lipid phase. In addition, it cannot be excluded that the probe binding kinetics is influenced by the lysozyme-induced lipid demixing and the dye lateral diffusion in the bilayer plane toward the PC-rich domains.

Taken together the results presented here clearly indicate that lysozyme possesses higher affinity for model membranes and exerts much more pronounced effect on structure and dynamics of lipid bilayer compared to ribonuclease A. The observed phenomenon cannot be interpreted as arising exclusively from the lower positive charge of the latter protein, since RNase exhibited weaker association also with the neutral membrane. What is the reason for the observed high membrane-binding ability for lysozyme? The answer to this question may lie in the structural peculiarities of the examined proteins. According to the theoretical predictions based on mean-field chain packing theory peptides containing amphipathic α-helices have stronger tendency to adsorb onto the membrane surface and thereafter to self-associate in membrane-bound state [87]. Analysis of lysozyme four α-helices showed that the helix including the residues Thr89-Gly102 is amphipathic (Fig. 9). This helix belongs to the helix-loop-helix domain (87–114 residues of Lz) located at the upper lip of the protein active site cleft which serves as an anchor upon lysozyme-membrane binding [39]. In contrast, as can be judged

Table 3
Kinetic parameters of SQ-1 binding to PC:CL (9:1) model membranes

System	I_{max}	τ_{eq}, min	χ^2
No protein	4.6±0.08	0.98±0.01	0.06
+Lz	13.9±0.5	10.68±0.1	0.02
+RNase	7.6±0.2	2.38±0.04	0.08

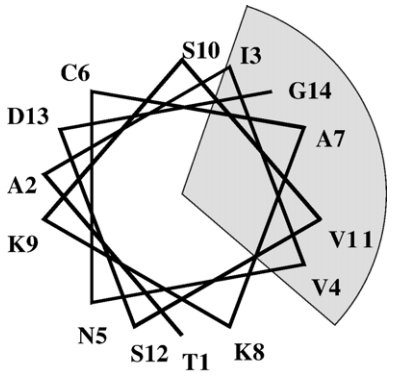

Fig. 9. Helical wheel diagram of lysozyme α-helix (residues Thr89–Gly102). Segregated hydrophobic residues in α-helical conformation are highlighted by grey shading. Radius of the unshaded sector subtends the protein polar angle.

from protein crystal structure, none of RNase α-helices is amphipathic. This dissimilarity in the structure of the proteins is likely to determine the higher lipid-associating and lipid-modulating abilities of lysozyme.

5. Conclusions

The present study represents the first report about the behavior of newly synthesized squarylium dye SQ-1 in lipid and protein–lipid systems. Moreover, the work offers new insights into the molecular details of lysozyme- and ribonuclease–lipid interactions. The results obtained indicate that squarylium dye SQ-1 readily binds to the proteins and model lipid membranes mainly *via* hydrophobic interactions. SQ-1 partitioning into the lipid and protein phases is followed by the increase of its fluorescence intensity without any shift of emission maximum. Negligible fluorescence of free SQ-1 and increase in emission upon binding makes it an ideal candidate for tracing the membrane- and protein-related processes. Lysozyme and ribonuclease were found to make impact on the probe association with model membranes resulting presumably from the competition between SQ-1 and the proteins for bilayer free volume and modification of the membrane structure and dynamical properties. Varying membrane composition provides evidence for the dye sensitivity to both hydrophobic and electrostatic protein–lipid interactions. The data presented here demonstrate that lysozyme affinity for the membrane is much higher than that of ribonuclease. This effect was supposed to originate mainly from the amphipathy of Lz α-helix involved in the membrane binding.

Fluorescence anisotropy measurements revealed the restriction of SQ-1 rotational mobility in lipid environment in the presence of Lz and RNase, thereby providing evidence for incorporation of the proteins into nonpolar region of lipid bilayer. Furthermore, the magnitude of this effect was found to increase with protein concentration and CL content. Extremely high Lz-induced increase in SQ-1 anisotropy in PC:CL (9:1) was supposed to arise from the aggregation of membrane-bound protein molecules.

Cumulatively, binding, fluorescence quenching and kinetic studies allowed us to assume that lysozyme induces lipid segregation upon association with negatively charged membranes

with threshold concentration of anionic lipid CL for the lipid demixing being 10 mol%. Furthermore, congregation of lipid molecules is suggested to occur in strictly defined range of *L*:*P* ratios at which electrostatic protein–lipid interactions essentially contribute to the protein-membrane binding. Lysozyme-induced lipid lateral separation in couple with the possibility of protein aggregation in membrane-bound state may have important functional implications in view of catalytic, bactericidal and amyloidogenic actions of this protein. The employment of new squarylium dye SQ-1 in membrane studies may prove of particular usefulness in monitoring protein–lipid interactions and related structural reorganization of lipid bilayer.

References

[1] S. May, D. Harries, A. Ben-Shaul, Lipid demixing and protein–protein interactions in the adsorption of charged proteins on mixed membranes, Biophys. J. 79 (2000) 1747–1760.

[2] N. Ben-Tal, B. Honig, C. Miller, S. McLaughlin, Electrostatic binding of proteins to membranes. Theoretical predictions and experimental results with charybdotoxin and phospholipid vesicles, Biophys. J. 73 (1997) 1717–1727.

[3] M. Sankaram, D. Marsh, Protein–lipid interactions with peripheral membrane proteins, Protein–Lipid Interactions, Elsevier, 1993, pp. 127–162.

[4] J. Kleinschmidt, J. Mahaney, D. Thomas, D. Marsh, Interaction of bee venom melittin with zwitterionic and negatively charged phospholipid bilayers: a spin-label electron spin resonance study, Biophys. J. 72 (1997) 767–778.

[5] F. Dumas, M. Lebrun, P. Peyron, A. Lopez, J. Tocanne, The transmembrane protein bacterioopsin affects the polarity of the hydrophobic core of the host lipid bilayer, Biochim. Biophys. Acta 1421 (1999) 295–305.

[6] M. Roux, Y. Newmann, R. Hodges, Conformational changes of phospholipid headgroups induced by a cationic integral membrane peptide as seen by deuterium magnetic resonance, Biochemistry 28 (1989) 2313–2321.

[7] C. Dempsey, M. Bitbol, A. Watts, Interaction of melittin with mixed phospholipid membranes composed of dimyristoylphosphatidylserine studied by deuterium NMR, Biochemistry 28 (1989) 6590–6595.

[8] Y. Babin, J. D'Amour, M. Pigeon, M. Pezolet, A study of the structure of polymyxin B — dipalmitoylphosphatidylglycerol complexes by vibrational spectroscopy, Biochim. Biophys. Acta 903 (1987) 78–88.

[9] G. Schwarz, G. Beschiachvili, Thermodynamic and kinetic studies on the association of melittin with a phospholipid bilayer, Biochim. Biophys. Acta 979 (1989) 82–90.

[10] M. Caffrey, G.W. Feigenson, Fluorescence quenching in model membranes: 3. Relationship between calcium adenosinetriphosphatase enzyme activity and the affinity of the protein for phosphatidylcholines with different acyl chain characteristics, Biochemistry 20 (1981) 1949–1961.

[11] Y. Takakuwa, C.G. Pack, X.L. An, S. Manno, E. Ito, M. Kinjo, Fluorescence correlation spectroscopy analysis of the hydrophobic interactions of protein 4.1 with phosphatidylserine liposomes, Biophys. Chemist. 82 (1999) 149–155.

[12] P.K.J. Kinnunen, A. Koiv, J.Y.A. Lehtonen, M. Rytomaa, P. Mustonen, Lipid dynamics and peripheral interactions of proteins with membrane surfaces, Chem. Phys. Lipids 73 (1994) 181–207.

[13] C.E. Caesar, E.K. Esbjorner, P. Lincoln, B. Norden, Membrane interactions of cell-penetrating peptides probed by tryptophan fluorescence and dichroism techniques: correlations of structure to cellular uptake, Biochemistry 45 (2006) 7682–7692.

[14] N. Kahya, Targeting membrane proteins to liquid-ordered phases: molecular self-organization explored by fluorescence correlation spectroscopy, Chem. Phys. Lipids 141 (2006) 158–168.

[15] E. Rhoades, T.F. Ramlall, W.W. Webb, D. Eliezer, Quantification of alpha-synuclein binding to lipid vesicles using fluorescence correlation spectroscopy, Biophys. J. 90 (2006) 4692–4700.

[16] V.M. Ioffe, G.P. Gorbenko, Lysozyme effect on structural state of model membranes as revealed by pyrene excimerization studies, Biophys. Chemist. 114 (2005) 199–204.

[17] P. Mattjus, J.G. Molotkovsky, J.M. Smaby, R.E. Brown, A fluorescence resonance energy transfer approach for monitoring protein-mediated glycolipid transfer between vesicle membranes, Anal. Biochem. 268 (1999) 297–304.

[18] M. Rytömaa, P.K.J. Kinnunen, Reversibility of the binding of cytochrome *c* to liposomes. Implications for lipid–protein interactions, J. Biol. Chem. 270 (1995) 3197–3202.

[19] X. Zhang, T.A. Keiderling, Lipid-induced conformational transitions of beta-lactoglobulin, Biochemistry 45 (2006) 8444–8452.

[20] A.A. Musse, J. Wang, G.P. Deleon, G.A. Prentice, E. London, A.R. Merrill, Scanning the membrane-bound conformation of helix 1 in the colicin E1 channel domain by site-directed fluorescence labelling, J. Biol. Chem. 281 (2006) 885–895.

[21] G.P. Gorbenko, Ye.A. Domanov, Cytochrome *c* location in phosphatidylcholine/cardiolipin model membranes: resonance energy transfer study, Biophys. Chemist. 103 (2003) 239–249.

[22] G.P. Gorbenko, Resonance energy transfer study of hemoglobin and cytochrome *c* complexes with lipids, Biochim. Biophys. Acta 1409 (1998) 12–24.

[23] E. Szczesna-Skorupa, B. Mallah, B. Kemper, Fluorescence resonance energy transfer analysis of cytochromes P450, 2C2 and 2E1 molecular interactions in living cells, J. Biol. Chem. 278 (2003) 31269–31276.

[24] F. Fernandes, L.M.S. Loura, M. Prieto, R. Koehorst, R.B. Spruijt, M.A. Hemminga, Dependence of M13 major coat protein oligomerization and lateral segregation on bilayer composition, Biophys. J. 85 (2003) 2430–2441.

[25] P.V. Nazarov, R.B. Koehorst, W.L. Vos, V.V. Apanasovich, M.A. Hemminga, FRET study of membrane proteins: simulation-based fitting for analysis of membrane protein embedment and association, Biophys. J. 91 (2006) 454–466.

[26] A.J. Mason, I.N. Chotimah, P. Bertani, B.A. Bechinger, A spectroscopic study of the membrane interaction of the antimicrobial peptide Pleurocidin, Mol. Membr. Biol. 23 (2006) 185–194.

[27] A.M. Powl, J. Carney, P. Marius, J.M. East, A.G. Lee, Lipid interactions with bacterial channels: fluorescence studies, Biochem. Soc. Trans. 33 (2005) 905–909.

[28] H. Zhao, E.K.J. Tuominen, P.K.J. Kinnunen, Formation of amyloid fibers triggered by phosphatidylserine-containing membranes, Biochemistry 43 (2004) 10302–10307.

[29] H. Zhao, A. Jutila, T. Nurminen, S.A. Wickstrom, J. Keski-Oja, P.K.J. Kinnunen, Binding of endostatin to phosphatidylserine-containing membranes and formation of amyloid-like fibers, Biochemistry 44 (2005) 2857–2863.

[30] J.R. Lakowicz, Principles of Fluorescent Spectroscopy, Plenum Press, New York, 1999.

[31] V.M. Ioffe, G.P. Gorbenko, A.L. Tatarets, L.D. Patsenker, E.A. Terpechnig, Examining protein–lipid interactions in model systems with a new squarylium fluorescent dye, J. Fluoresc. 16 (2006) 547–554.

[32] D. Keil, H. Hartmann, T. Moschny, Synthesis and characterization of 1,3-bis-(2-dialkylamino-5-thienyl)-substituted squaraines — a novel class of intensively coloured panchromatic dyes, Dyes Pigm. 17 (1991) 19–27.

[33] D. Ramaiah, I. Eckert, K.T. Arun, L. Weidenfeller, B. Epe, Squaraine dyes for photodynamic therapy: mechanism of cytotoxicity and DNA damage induced by halogenated squaraine dyes plus light (>600 nm), Photochem. photobiol. 79 (2004) 99–104.

[34] K.Y. Law, F.C. Bailey, Squaraine chemistry: effect of synthesis on the morphological and xerographic properties of photoconductive squaraines, J. Imag. Sci. 31 (1987) 172–175.

[35] Polaroid Corporation, US Patent 5795981.

[36] V.Y. Merritt, H.J. Hovel, Organic solar cells of hydroxysquarylium, Appl. Phys. Lett. 29 (1976) 414–416.

[37] H.R. Ibrahim, M. Yamada, K. Matsushita, K. Kobayashi, A. Kato, Enhanced bactericidal action of lysozyme to *Escherichia coli* by inserting a hydrophobic pentapeptide into its C terminus, J. Biol. Chem. 269 (1994) 5053–5063.

[38] A. Pellegrini, U. Thomas, N. Bramaz, S. Klauser, P. Hunziker, R. von Fellenberg, Identification and isolation of a bactericidal domain in chicken egg white lysozyme, J. Appl. Microbiol. 82 (1997) 372–378.

[39] H.R. Ibrahim, U. Thomas, A. Pellegrini, A helix-loop-helix peptide at the upper lip of the active site cleft of lysozyme confers potent antimicrobial activity with membrane permeabilization action, J. Biol. Chem. 276 (2001) 43767–43774.
[40] R.T. Raines, Ribonuclease A, Chem. Rev. 98 (1998) 1045–1065.
[41] P.A. Leland, L.W. Schultz, B.M. Kim, R.T. Raines, Ribonuclease A variants with potent cytotoxic activity, Proc. Natl. Acad. Sci. U. S. A. 95 (1998) 10407–10412.
[42] H.K. Kimelberg, D. Papahadjopoulos, Interactions of basic proteins with phospholipid membranes. Binding and changes in the sodium permeability of phosphotidylserine vesicles, J. Biol. Chem. 246 (1971) 1142–1148.
[43] L. Stryer, Biochemistry, W.H. Freeman, New York, 1995.
[44] H.K. Kimelberg, Protein–liposome interactions and their relevance to the structure and function of cell membranes, Mol. Cell. Biochem. 10 (1976) 171–190.
[45] D.D. Pless, W.J. Lennarz, Enzymatic conversion of proteins to glycoproteins, Proc. Natl. Acad. Sci. U. S. A. 74 (1977) 134–138.
[46] M. Stefani, Protein misfolding and aggregation: new examples in medicine and biology of the dark side of the protein world, Biochim. Biophys. Acta 1739 (2004) 5–25.
[47] L.C. Serpell, Alzheimer's amyloid fibrils: structure and assembly, Biochim. Biophys. Acta 1502 (2000) 16–30.
[48] E. Terzi, G. Höelzemann, J. Seelig, Alzheimer Aβ-amyloid peptide 25–35: electrostatic interactions with phospholipid membranes, Biochemistry 33 (1994) 7434–7441.
[49] G.P. Gorbenko, P.K.J. Kinnunen, The role of lipid–protein interactions in amyloid-type protein fibril formation, Chem. Phys. Lipids 141 (2006) 72–82.
[50] A. Cao, D. Hu, L. Lai, Formation of amyloid fibrils from fully reduced hen egg white lysozyme, Protein Sci. 13 (2004) 319–324.
[51] M. Dumoulin, D. Canet, A.M. Last, E. Pardon, D.B. Archer, S. Muyldermans, L. Wyns, A. Matagne, C.V. Robinson, C. Redfield, C.M. Dobson, Reduced global cooperativity is a common feature underlying the amyloidogenicity of pathogenic lysozyme mutations, J. Mol. Biol. 346 (2005) 773–788.
[52] S. Sambashivan, Y. Liu, M.R. Sawaya, M. Gingery, D. Eisenberg, Amyloid-like fibrils of ribonuclease A with three-dimensional domain-swapped and native-like structure, Nature 437 (2005) 266–269.
[53] M.H. Filgueiras, J.A. Op den Kamp, Cardiolipin, a major phospholipid of Gram-positive bacteria that is not readily extractable, Biochim. Biophys. Acta 620 (1980) 332–337.
[54] Q. Li, T. Ji, P. Bi-Xian, Synthesis and characterization of heptamethine cyanine dyes, Molecules 2 (1997) 91–98.
[55] S.H. Kim, S.H. Hwang, J.J. Kim, C.M. Yoon, S.R. Keun, Synthesis and properties of functional aminosquarylium dyes, Dyes Pigm. 37 (1998) 145–154.
[56] B. Mui, L. Chow, M.J. Hope, Extrusion technique to generate liposomes of defined size, Methods Enzymol. 367 (2003) 3–14.
[57] G. Bartlett, Phosphorus assay in column chromatography, J. Biol. Chem. 234 (1959) 466–468.
[58] J.C. Cheetham, P.J. Artymiuk, D.C. Phillips, Refinement of an enzyme complex with inhibitor bound at partial occupancy. Hen egg-white lysozyme and tri-*N*-acetylchitotriose at 1.75 Å resolution, J. Mol. Biol. 224 (1992) 613–628.
[59] R.F. Tilton, J.C. Dewan, G.A. Petsko, Effects of temperature on protein structure and dynamics: X-ray crystallographic of the protein ribonuclease A at nine different temperatures from 98 to 320 K, Biochemistry 31 (1992) 2469–2481.
[60] N.C. Santos, M. Prieto, M.A.R.B. Castanho, Quantifying molecular partition into model systems of biomembranes: an emphasis on optical spectroscopic methods, Biochim. Biophys. Acta 1612 (2003) 123–135.
[61] V.G. Ivkov, G.N. Berestovsky, Dynamic Structure of Lipid Bilayer, Nauka, Moscow, 1981.
[62] C.R. Cantor, P.R. Schimmel, Biophysical Chemistry, San Francisco, 1984.
[63] B. Oswald, F. Lehmann, L. Simon, E. Terpetschnig, O.S. Wolbeis, Red laser-induced fluorescence energy transfer in an immunosystem, Anal. Biochem. 280 (2000) 272–277.
[64] B. Valeur, Molecular Fluorescence. Principles and Applications, Wiley-VCH, New York, 2001.
[65] A. Shibata, K. Ikawa, T. Shimooka, H. Terada, Significant stabilization of the phosphatidylcholine bilayer structure by incorporation of small amounts of cardiolipin, Biochim. Biophys. Acta 1192 (1994) 71–78.
[66] T. Gulik-Krzywicki, E. Shechter, V. Luzzati, M. Faure, Interactions of proteins and lipids: structure and polymorphism of protein–lipid–water phases, Nature 223 (1969) 1116–1120.
[67] E. Posse, B.F. de Arcuri, d.R.D. Morero, Lysozyme interactions with phospholipid vesicles: relationships with fusion and release of aqueous content, Biochim. Biophys. Acta 1193 (1994) 101–106.
[68] O. Zschornig, G. Paasche, C. Thieme, N. Korb, K. Arnold, Modulation of lysozyme charge influences interaction with phospholipid vesicles, Colloids Surf., B Biointerfaces 42 (2005) 69–78.
[69] M.N. Dimitrova, H. Matsumura, N. Terezova, V. Neytchev, Binding of globular proteins to lipid membranes studied by isothermal titration calorimetry and fluorescence, Colloids Surf. B Biointerfaces 24 (2002) 53–61.
[70] D. Papahadjopoulos, M. Moscarello, E.H. Eylar, T. Isac, Effects of proteins on thermotropic phase transitions of phospholipid membranes, Biochim. Biophys. Acta 401 (1975) 317–335.
[71] Y.L. Lo, Y.E. Rahman, Protein location in liposomes, a drug carriers: a prediction by differential scanning calorimetry, J. Pharm. Sci. 84 (1995) 805–814.
[72] A. Raudino, F. Castelli, A thermodynamic study of protein–lipid lateral phase separation. Effect of lysozyme on mixed lipid vesicles, Colloid Polym. Sci. 270 (1992) 1116–1123.
[73] G. Denisov, S. Wanaski, P. Luan, M. Glaser, S. McLaughlin, Binding of basic peptides to membranes produces lateral domains enriched in the acidic lipids phosphatidylserine and phosphatidylinositol 4,5-bisphosphate: an electrostatic model and experimental results, Biophys. J. 74 (1998) 731–744.
[74] O. Zschornig, G. Paasche, C. Thieme, N. Korb, A. Fahrwald, K. Arnold, Association of lysozyme with phospholipid vesicles is accompanied by membrane surface dehydration, Gen. Physiol. Biophys. 19 (2000) 85–101.
[75] P.J.K. Kinnunen, On the principles of functional ordering in biological membranes, Chem. Phys. Lipids 57 (1991) 375–399.
[76] F. Liu, I.P. Sugar, L.G. Chong, Cholesterol and ergosterol superlattices in three-component liquid crystalline lipid bilayers as revealed by dehydroergosterol fluorescence, Biophys. J. 72 (1997) 2243–2254.
[77] B.F. de Arcuri, G.F. Vechetti, R.N. Chehin, F.M. Goni, R.D. Morero, Protein-induced fusion of phospholipid vesicles of heterogeneous sizes, Biochem. Biophys. Res. Commun. 262 (1999) 586–590.
[78] M. Ge, J.H. Freed, Hydration, structure, and molecular interactions in the headgroup region of dioleoylphosphatidylcholine bilayers: an electron spin resonance study, Biophys. J. 85 (2003) 4023–4040.
[79] M. Vedamuthu, S. Singh, Y. Onganer, D.R. Bessire, M. Yin, E.L. Quitevis, G.W. Robinson, Universality in isomerization reactions in polar solvents, J. Phys. Chem. 100 (1996) 11907–11913.
[80] F. Momicchioli, A.S. Tatikolov, D. Vanossi, G. Ponterini, Electronic structure and photochemistry of squaraine dyes: basic theoretical analysis and direct detection of the photoisomer of a symmetrical squarylium cyanine, Photochem. photobiol. Sci. 3 (2004) 396–402.
[81] M.A. Haidekker, T. Brady, K. Wen, C. Okada, H.Y. Stevens, J.M. Snell, J.A. Frangos, E.A. Theodorakis, Phospholipid-bound molecular rotors: synthesis and characterization, Bioorg. Med. Chem. 10 (2002) 3627–3636.
[82] S. Paula, A.G. Volkov, D.W. Deamer, Permeation of halide anions through phospholipid bilayers occurs by the solubility–diffusion mechanism, Biophys. J. 74 (1998) 319–327.
[83] J.R. Lakowicz, D. Hogen, Chlorinated hydrocarbon-cell membrane interactions studied by the fluorescence quenching of carbazole-labeled phospholipids: probe synthesis and characterization of the quenching methodology, Chem. Phys. Lipids 26 (1980) 1–40.
[84] S.J. Marrink, H.J.C. Berendsen, Simulation of water transport through a lipid membrane, J. Phys. Chem. 98 (1994) 4155–4168.
[85] R.T. Hamilton, E.W. Kaler, Facilitated ion transport through thin bilayers, J. Membr. Sci. 54 (1990) 259–269.
[86] G.E. Dobretsov, Fluorescent Probes in Investigation of Cells, Membranes and Lipoproteins, Nauka, Moscow, 1989.
[87] A. Zemel, S. Ben-Shaul, May, Membrane perturbation induced by interfacially absorbed peptides, Biophys. J. 86 (2004) 3607–3619.